INTERPRETATION OF CORONAL SYNOPTIC OBSERVATIONS

Richard H. Munro and Richard R. Fisher

High Altitude Observatory, National Center for Atmospheric Research, Boulder, CO

I. INTRODUCTION

Three-dimensional reconstruction techniques used to determine coronal density distributions from synoptic data are complicated and time consuming to employ. Current techniques also assume time invariant structures and thus mix both temporal and spatial variations present in the coronal data. The observed distribution of polarized brightness, pB, and brightness, B, of coronal features observed either at eclipses or with coronagraphs depends upon both the three-dimensional distribution of electron density within the structure and the location of the feature with respect to the plane-of-the-sky. By theoretically studying the signature of various coronal structures as they would appear during a limb transit, it is possible to recognize these patterns in real synoptic data as well as estimate temporal evolutionary effects.

II. TIME INDEPENDENT MODELS

Coronal streamers, large-scale white-light structures found in the solar corona, are the most impressive and easily observed features of the extended solar atmosphere. In the summer of 1984, a period in which there were few structures associated with solar active regions, the corona was dominated by streamers associated with the large-scale solar magnetic field. Rotating more rigidly than the photospheric material, several streamers were observed near the solar limbs on DOY 222 with both the spacecraft and ground based instruments. For this investigation, only the distribution of polarized brightness (pB), at a reference height of 1.3 $R_\odot$, over latitude and longitude has been used to estimate a model-dependent electron density at the base of these streamers. Portions of the K-coronameter synoptic record are shown in Figure 1.

The investigation of the gross brightness properties of the solar corona does not require a detailed model of the density structure. Thus we have chosen to represent coronal features using simple "ad hoc" mathematical descriptions. Coronal streamers are assumed to be radial features with circular cross sections that depend on radius. The bottom portion of "helmet-like" shape (increasing then decreasing cross-sectional projection) was obtained from eclipse measurements. The cross-sectional area is set to a constant above a given height (~2.5 $R_\odot$). At 1.3 $R_\odot$, the angular width of the streamer measured from Sun center is 15 degrees. For these calculations, the density structure within the streamer has the identical radial logarithmic gradient as the surrounding background, but with a constant enhancement over the background (corresponding to an increased base pressure). Model streamers were placed in solar longitude and latitude at the corresponding brightness maxima of the observations.

Note that during the period of these observations, the large-scale corona contained six bright regions or streamers. On DOY 222, two of these were located in the southern hemisphere on the east limb, two were located near the plane-of-the-sky on the west limb in the northern hemisphere, and the remaining two streamers, somewhat fainter than the others, spanned the equator near the center of the disk.

An equatorial symmetric background corona was initially used to determine a multiplier to the Allen (1963) Minimum Model to replicate the observed polarized brightness between the streamers at 1.3 $R_\odot$. The streamer enhancements required to match the observed maximum polarized brightnesses for each structure averaged 3.1 times the equatorial background. This enhancement in streamer density required is, of course, dependent upon the specific model geometry given above, and is only a sufficient model. Taken at face value, a mean density of 5.6 x 10^7 electrons cm^{-3} in the streamer is obtained at the reference height. The ratio of streamer pB to the background corona is roughly the same as that found by Wilson (1977). On the other hand, the absolute density for the entire corona is about a factor of 2 lower than the extrapolated value obtained from Wilson's study. Estimates of the expected polarized brightness distribution (Fig. 2), obtained by using the model density distribution, replicate the observed distribution of polarized brightness with reasonable fidelity.

III. SIGNATURES OF STREAMERS IN K-CORONAMETER DATA

The major features found in the observed synoptic chart (Fig. 1) from the east and west limb data are reproduced (Fig. 2), providing insight into the effects of the long integration path through the corona and the variation of the apparent location of the streamer as a function of solar rotation. Thus, it is clear that this relatively simple modeling technique allows the rapid interpretation of K-coronameter and coronagraph results, at least in the case of the largest features found in the solar corona. However, some of the characteristic signatures displayed in the model are absent in the data. The dashed lines on the observed synoptic chart mark the theoretical track of the two streamers closest to the solar poles. While the southern streamer matches the model calculations, a glaring discrepancy exists for the northern-most high-latitude streamer. In this case, the data do not display a symmetric feature, but rather a strange trailing extension from the maximum polarization brightness region (time runs right to left in coronal synoptic maps). To gain insight into this problem, synoptic observations from the three HAO K-coronameters covering the years 1965-1984 were used to classify the signature of streamers as they appeared during limb passage. The shape categories included round, trailing extensions, leading extensions, symmetric extensions, and other complex features. The results are summarized in Table 1. Although it is possible to construct static models of coronal density distributions that produce the observed shape of the extensions, round coronal signatures cannot be produced by a static structure.

Emerging from an examination of a long-term synoptic record is the perception that while the underlying organization of the large-scale photospheric magnetic field tends to be quite persistent, at least one-third of the streamers identified in K-coronameter synoptic charts must evolve with a timescale approximately equal to the length of time such a structure is visible using coronagraphic techniques. Taking this argument further, the overwhelming number of trailing extensions over leading extensions implies that the temporal scales for injecting material into a streamer are shorter than for removing the material.

IV. TIME DEPENDENT MODELS

To investigate how time-dependent density enhancements and reductions might appear in synoptic observations, the model streamers described above were subjected to linear rates of formation and destruction. Figure 3 depicts sample signatures for streamers at a latitude of 45 degrees North where the maximum density for the streamers occurs one day after, at, and one day

before limb passage for the top, middle and bottom panels, respectively. With each panel, the model streamers form in one day, but decay in one, two, three, and four days. The signatures for slow formation and rapid decay are mirror images of these forms about the central time of the individual panels (or 90 degrees longitude).

These calculations show that:

(1) The absence of an extension implies rapid density variations and "round" signatures require both rapid injection and removal of material.

(2) The location of the observed maximum brightness depends on the time when the streamer attained its maximum density, and only weakly on the spatial location of the streamer. The physical location of the streamer remained constant in the models displayed in Figure 3; only the time of maximum density was allowed to vary. As a rule of thumb, the observed maximum brightness signals the time of maximum density within 8 hours as long as the peak density was attained within 2 days of the streamer's limb passage. Thus, caution must be used when associating the physical location of streamers as determined by synoptic observations with underlying photospheric features.

(3) The shape of the brightness distribution of an observed streamer can provide clues as to the nature of the temporal evolution of streamer material. This variation can be seen by selecting a particular injection and removal rate (e.g., 1:4, the lower right of each panel), and comparing the signatures as the time of peak density varies from after (top) to before (bottom) limb passage.

REFERENCES

Allen, C. W., 1963, in *Astrophysical Quantities,* University of London, London, p. 176.

Wilson, D. C., 1977, *The Three Dimensional Solar Corona – A Coronal Streamer,* NCAR Cooperative Thesis No. 40, National Center for Atmospheric Research, Boulder, Colorado.

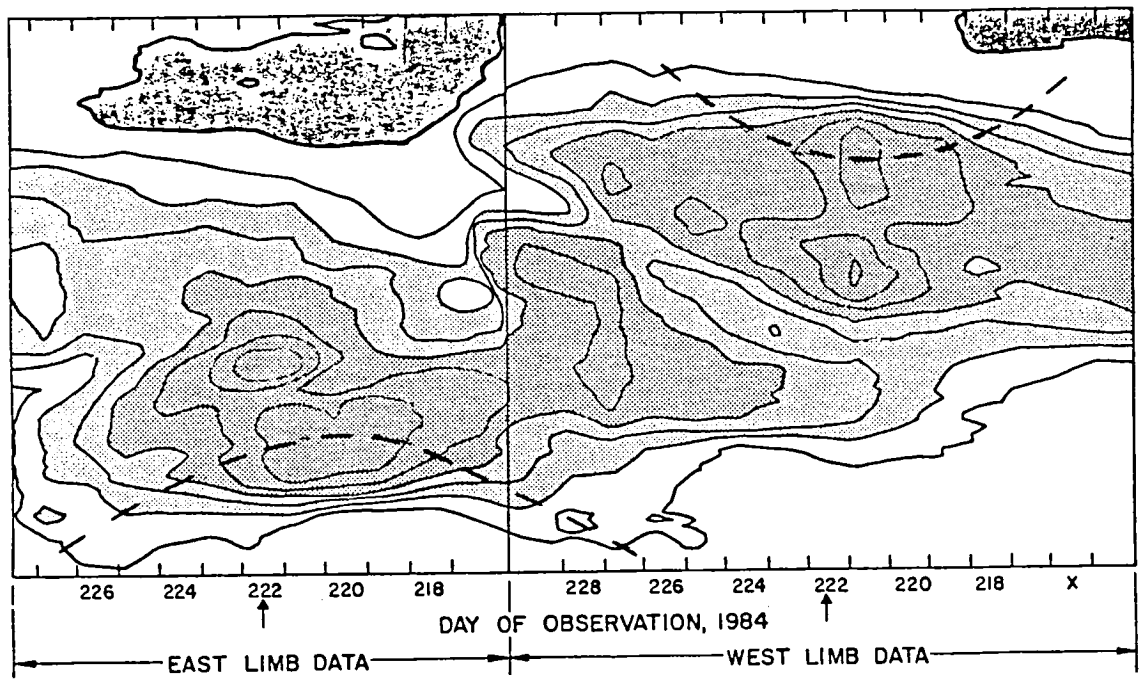

Figure 1. Portions of the K-coronameter synoptic record, from both the east and west limbs, centered on DOY 222 1984. Amplitude of the polarized brightness of the corona is plotted as a function of solar latitude and day of observation. Dashed lines mark the theoretical track of the northern-most and southern-most streamers.

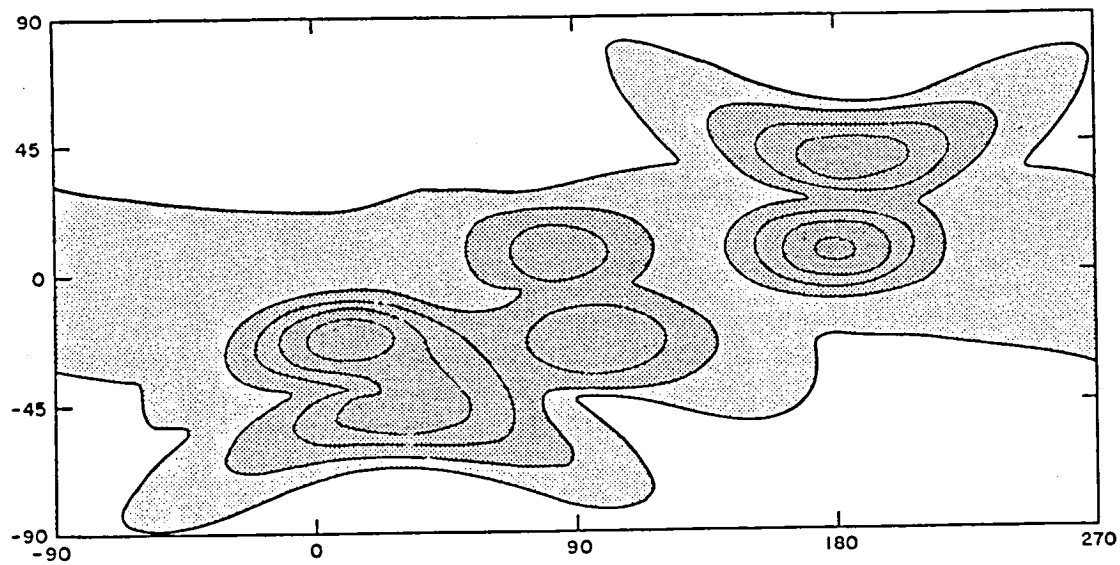

Figure 2. The estimated polarized brightness that would be observed from the earth if material were distributed over the volume of the corona in accordance with a model that has (1) a quiet background contribution, the axis of symmetry which is tilted with respect to the solar rotation axis, and (2) six embedded streamers with the geometrical properties given in the model (see text). The streamer densities have been adjusted so as to achieve the observed peak polarized brightness.

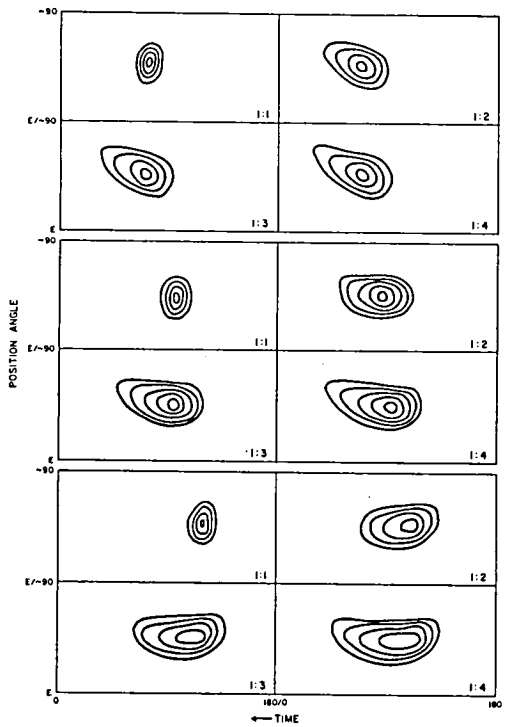

Figure 3. Synoptic observational signatures of time-dependent model streamers with varying rates of material removal and time of maximum density enhancement. (See text for additional information.)

TABLE 1. OBSERVED STREAMER SIGNATURES IN THE HAO K-CORONAMETERS 1965–1984

	Stationary	Obvious Temporal Evolution			Sum	Other, Complex Features	Total
		Round	Trailing Extension	Leading Extension			
Number	77	250	412	57	796	1131	1927
Fraction	4%	13%	21%	3%	41%	59%	100%
Fraction	10%	31%	52%	7%	100%		